PHYSICAL REVIEW B VOLUME 35, NUMBER 5 15 FEBRUARY 1987-I

Time-resolved photoluminescence of dense electron-hole plasmas in In-Ga-As-P films

A. J. Taylor* and J. M. Wiesenfeld
AT&T Bell Laboratories, Crawford Hill Laboratory, Holmdel, New Jersey 07733
(Received 5 May 1986)

Time-resolved photoluminescence spectra of dense electron-hole plasmas in In-Ga-As-P films have been measured with 200-ps resolution, at room temperature. The carrier density, temperature, and band-gap energy are determined as a function of time delay following excitation and of initially excited carrier density. We observe the theoretically predicted band-gap renormalization. The carrier temperature is found to equilibrate to a temperature near the lattice temperature within 200 ps after excitation. Initially photoexcited carrier densities of more than 5×10^{20} cm^{-3} are found to decay to less than 6×10^{18} cm^{-3} within 200 ps. Evidence is presented which indicates that expansion of the electron-hole plasma is an important mechanism in this decay. The density decay after 200 ps is due to a combination of Auger and radiative recombination.

I. INTRODUCTION

Using time-resolved photoluminescence techniques, experiments that study the carrier dynamics of high-density electron-hole plasmas in the quaternary semiconductor In-Ga-As-P are reported. In particular, we examine the time evolution of the photoluminescence spectra due to the very dense electron-hole plasmas created by optical excitation with subpicosecond pulses. The study of carrier dynamics in In-Ga-As-P alloys is not only of fundamental interest, but is important for the design of the optoelectronic devices that are relevant to optical communication technology. Only a few experiments[1-5] have, to our knowledge, previously studied the time-resolved luminescence from these materials. However, none of these studies focused on the high-density regime, where nonradiative decay mechanisms and many-body processes should be relevant. It is the purpose of this paper to examine the carrier dynamics in the high-density electron-hole plasma, and, in particular, to elucidate the competition between plasma expansion and Auger recombination, both of which are observed in the present experiments. This high-density regime is also important for understanding the behavior of optically pumped In-Ga-As-P film lasers.[6]

From our data, which consists of room-temperature luminescence spectra taken at various time delays after excitation (with 200-ps resolution) and at a series of initially photoexcited carrier densities, we can make the following statements: By 200 ps after excitation, the carriers have equilibrated to a temperature near the lattice temperature. We observe band-gap renormalization behavior that agrees with the theory of Brinkman and Rice.[7] A rapid decay of the density from $>10^{20}$ cm^{-3} to 5×10^{18} cm^{-3} is observed during the first 200 ps after excitation. We find evidence indicating that rapid expansion of the electron-hole plasma[8-14] is an important mechanism in this decay. To verify the feasibility of this hypothesis, model rate equations for this system are solved and the results are compared with our data. The density decay after 200 ps is dominated by a combination of Auger and radiative recombination. We do not observe the narrow spectral linewidths of Ref. 2, indicating that our sample does not exhibit localization of electronic states.

II. EXPERIMENTAL SETUP

The samples studied were thin In-Ga-As-P films grown by liquid-phase epitaxy, lattice matched to InP. The free In-Ga-As-P film, obtained by etching away the InP, was then sandwiched between a microscope slide and a cover slip with epoxy. We studied 0.2- and 0.6-μm-thick films of $In_{0.70}Ga_{0.30}As_{0.66}P_{0.34}$ ($\lambda_g\approx1.3$ μm, where λ_g is the wavelength of the room-temperature band gap) and a 0.5-μm-thick film of $In_{0.58}Ga_{0.42}As_{0.93}P_{0.07}$ ($\lambda_g\approx1.5$ μm), and observed the same qualitative behavior in all samples. Unless otherwise stated, the data discussed here is for the 0.2-μm In-Ga-As-P sample.

Carriers in the semiconductor films are excited high above the band gap by 0.5-ps, 2-nJ pulses at 0.625 μm from a cavity-dumped, passively mode-locked, cw ring dye laser operating at a 200-kHz repetition rate. The laser output is chopped and focused onto the sample. The photoexcited carrier density in the samples is changed from 10^{18} to 5×10^{20} cm^{-3} by changing the laser intensity using a variable neutral-density filter, for two different focused-laser-beam diameters: 5 and 26 μm. The crystal has transverse dimensions of about 250 μm, which is much larger than the focal spot size. The luminescence transmitted through the film is collected and collimated with a 20× microscopic objective and focused through a monochromator with a 5× microscope objective. The spectrally filtered light from the monochromator is collected with a 5× microscope objective and then focused on a fast Ge avalanche photodiode (APD), which has a 200-ps impulse response time (full width at half maximum). Care has been taken to insure that the collected luminescence beam is not aperatured after the first collimating lens. The signal is amplified and then sampled at a fixed delay from the exciting pulse by a sampling oscilloscope operating in boxcar averaging mode. The resulting temporal resolution is 200 ps and the spectral reso-

lution of the monochromator is set to 6 nm. The output from the oscilloscope is synchronously detected and sent to a multichannel analyzer that is scanned in conjunction with the monochromator. This produces a luminescence spectrum for a certain initially photoexcited carrier density taken at a given delay from the excitation pulse. The luminescence spectra are analyzed on a microcomputer. We are able to obtain from these spectra the carrier density, band gap, and luminescence intensity as a function of delay and initial carrier density.

The initial density of photoexcited electron-hole pairs, N_0, is

$$N_0=\frac{1.3}{\pi\omega^2}\frac{E}{h\nu}(1-R)\left[\frac{1-e^{-\alpha d}}{d}\right], \quad (1)$$

where E is the energy of the excitation pulse, $h\nu$ is the photon energy at $\lambda=0.625$ μm, and R is the reflection coefficient. The absorption coefficient α at $\lambda=0.625$ μm is 7.5×10^4 cm^{-1}.[15] The factor of 1.3 converts the Gaussian initial distribution of carriers to an effective uniform density.[5] The laser spot size ω is determined from transmission measurements through a series of calibrated pinholes, assuming a Gaussian beam. It is assumed in Eq. (1) that the plasma expands uniformly to fill the submicron-thick film of thickness d on a time scale of ~1 ps. Because of this rapid plasma expansion, the luminescence collected in transmission is equivalent to that collected in reflection, as verified experimentally. Equation (1) assumes that every absorbed photon creates an electron-hole pair. This is valid for the present experimental conditions, since there is no evidence for nonlinear absorption of the $\lambda=0.625$ μm light.

Two types of series of spectra are recorded: (1) At a fixed photoexcited carrier density a series of spectra are taken, each at a different delay from the excitation pulse, and (2) at a delay of 200 ps (the minimum delay allowed by the system's temporal resolution) a series of spectra are taken, each with a different initially photoexcited carrier density. Extreme care was taken experimentally to insure that no other parameters were changed during the series of scans other than the one being varied. The first series

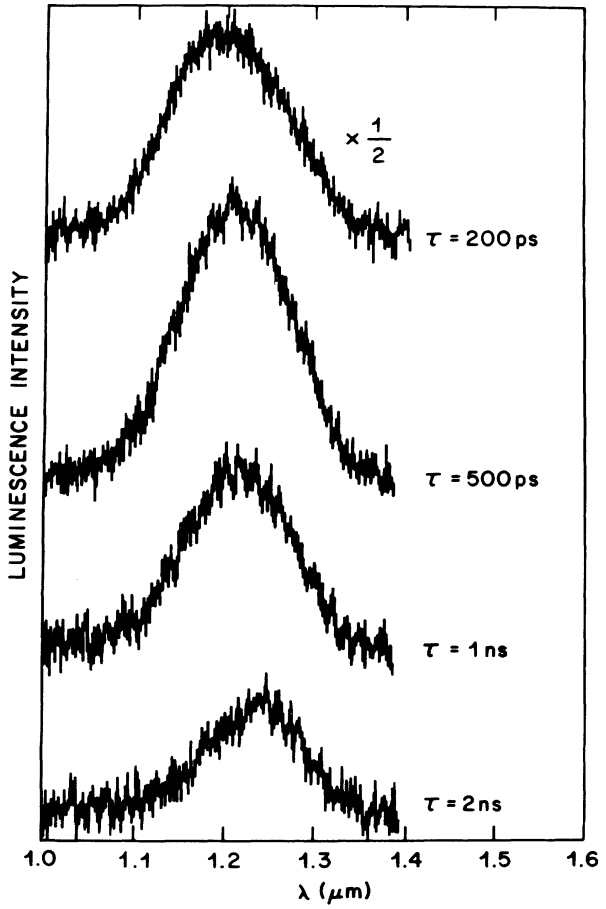

FIG. 1. A series of luminescence spectra, $L(\lambda)$ vs λ, each taken at a fixed initially photoexcited carrier density $N_0=2.6\times10^{19}$ cm^{-3}, but at a different delay τ from the excitation pulse. The initial spot diameter is 26 μm.

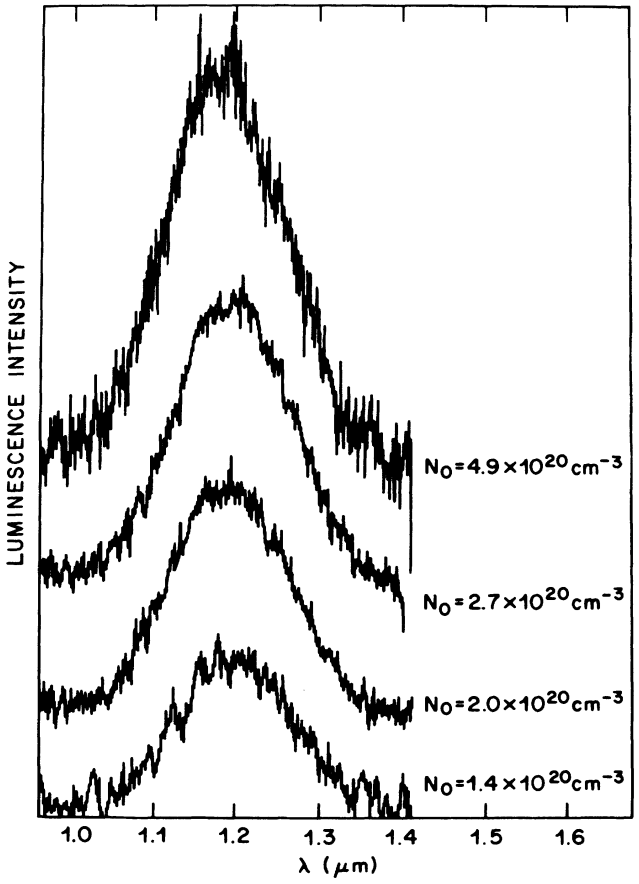

FIG. 2. A series of luminescence spectra, $L(\lambda)$ vs λ, each taken at a fixed delay $\tau=200$ ps from the excitation pulse, but at a different initial photoexcited carrier density N_0. The initial spot diameter is 5 μm.

of luminescence scans shows the temporal evolution of the carrier density. The second series yields the relative quantum efficiency of the decay process as a function of initial carrier density, and thus reflects the importance of the different density-dependent mechanisms such as Auger and bimolecular recombination and plasma expansion, during the first 200 ps after excitation. To extend the possible range of excitation densities without sacrificing signal, as well as to elucidate the importance of plasma expansion, a series of scans was taken with a 5-μm-diameter initially photoexcited spot and another series with a 26-μm-diameter spot. Figure 1 displays the first type of series taken with a 26-μm-diameter photoexcitation spot while Fig. 2 presents the second type taken with a 5-μm spot.

III. SPECTRAL ANALYSIS

The line shape of each experimental luminescence spectrum, $L(E)$ versus E is analyzed to determine the carrier density N, the band gap E_g, the carrier temperature T, and the relative amount of luminescence L_0 at a given time delay from the excitation pulse. Here we assume that the luminescence spectra result from the recombination of free electrons and holes. The theoretical spectral line shape, assuming k conservation during the photoemission process, can be calculated using Fermi's golden rule.

Kane's $\mathbf{k}\cdot\mathbf{p}$ model[16] is assumed for the band structure of In-Ga-As-P with the following parameters: electron mass in the Γ valley $m_\Gamma = 0.0605 m_0$,[17] nonparabolicity in the Γ valley $\alpha_\Gamma = 0.968$ eV^{-1}, heavy-hole mass $m_h = 0.5 m_0$,[18] light-hole mass $m_l = 0.072 m_0$,[19] spin-orbit splitting $\Delta = 0.25$ eV,[20] Γ-L valley splitting in the conduction band $E_{\Gamma L} = 0.55$ eV,[21] electron mass in the L valley $m_L = 0.328 m_0$,[17] and nonparabolicity in the L valley $\alpha_L = 0.634$ eV^{-1} (Ref. 17) (m_0 is the electron mass). Other values for some of the band-structure parameters have been reported.[22] Use of alternative values for the band-structure parameters can cause up to 10% uncertainty in our calculated results. The band-gap energy E_g was left as a parameter in the line-shape expression so that its dependence on carrier density could be derived from the data. The X valley was not included since it lies too far above the bottom of the conduction band to be populated even at the high carrier densities excited in this experiment. The matrix element M for the transition is obtained from Kane's formalism.[16]

Even at the highest excitation densities we observe spectral widths which correspond to densities of $\leq 6\times 10^{18}$ cm^{-3}. At these densities, it is reasonable to use a parabolic approximation for the conduction band, to neglect the L valley, and to neglect transitions from the light-hole and split-off valence bands. In this case the amount of luminescence of energy E impinging on the detector, $L(E)$, is

$$L(E) = L_0 E^3 M^2(E,E_g)(E-E_g)^{1/2} \times f_e(E-E_g,N,T) f_h(E-E_g,N,T) , \quad (2)$$

where f_e (f_h) is the Fermi function for the electrons (holes). Since expansion of the plasma is completed before the earliest time of observation, 200 ps (*vide infra*), it is unnecessary to consider displaced Fermi functions.[14] We fit each luminescence spectrum to Eq. (2) where N, E_g, L_0, and T are free parameters in the fit. Only the variation of L_0 over a series of spectra is determined, not its absolute magnitude.

Good fits of $L(E)$ to the data were obtained with $T = 300$ K for all levels of excitation. Substantially worse fits resulted for $T > 500$ K. For comparison, Fig. 3(a) shows a typical spectrum (dotted line) with the best fitting $L(E)$ curve at $T = 300$ K (solid line), while Fig. 3(b) shows the same spectrum fit with the best fitting $L(E)$ at $T = 500$ K. This implies that, although the initially photoexcited temperature may be as high as 4000 K, the plasma cools to approximately the lattice temperature in less than 200 ps. For all further analysis, a carrier temperature of 300 K has been assumed.

With the temperature fixed at 300 K there are three free parameters: N, E_g, and L_0. The parameters are fairly independent of one another, however, with N corresponding to the width of the spectrum, E_g to the position of the peak, and L_0 to the overall amplitude of the spectrum. The mismatch between the theoretical and experimental curves at low energies in Fig. 3(a) is caused by the absence of band tails in the theoretical expression for the density of states and the matrix element M. However, this discrepancy should not substantially affect the values of the parameters obtained from the data as the mismatch occurs over less than 10% of the spectrum.

In using Eq. (2) to describe the line shape of the luminescence, we assume that the luminescence is not

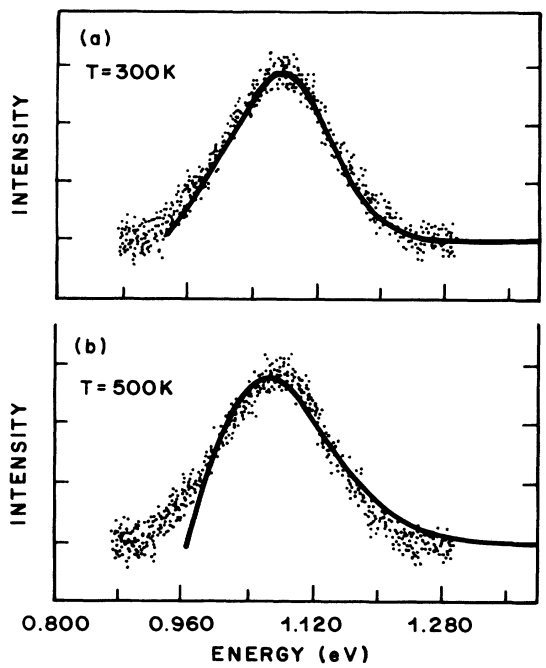

FIG. 3. Typical experimental luminescence spectra (points) with the best fitting curve $L(E)$ (solid line) for $T = 300$ K (a), and $T = 500$ K (b).

modified by absorption within the thin film.[23] This assumption is justified since the film is less than one absorption length thick at the wavelengths for which luminescence is observed. We estimate that this effect would contribute less than 10% change to the line-shape analysis.

IV. RESULTS AND DISCUSSION

All the observed spectra exhibit linewidths of ≈ 100 meV which decrease with increasing time delay. Physically reasonable values for N and E_g result from the spectral line-shape analysis. Therefore, our assumption that the recombination of electrons and holes is the dominant mechanism producing the luminescence is reasonable. These observations are in contrast to those of an earlier report[2] where time-resolved luminescence from In-Ga-As-P films of similar stoichiometry and photoexcited density was also measured. The authors of Ref. 2 report extremely narrow spectral linewidths of ≈ 10 meV which do not change with time delay. This behavior is attributed to luminescence from quasilocalized states caused by significant alloy fluctuations in the quaternary alloy semiconductor. Our spectra indicate that such alloy fluctuations are not fundamental to all quaternary samples.

A. Long-time decay

Consider the series of scans shown in Fig. 1 taken at delays of 200 ps to 3 ns for an initial photoexcited carrier density of 2.6×10^{19} cm^{-3} in a 26 μm diameter spot. From these scans the time evolution of the carrier density is found, as shown in Fig. 4. The density at a delay of 200 ps is 5.8×10^{18} cm^{-3}. Both Auger recombination and bimolecular radiative recombination will contribute to the subsequent density decay.[4,5,24–26] In this density regime the radiative recombination rate is slightly saturated,[27] resulting in a density dependent bimolecular rate constant of the form $B=B_0-B_1N$. Therefore, the data of Fig. 4 is analyzed according to the equation:

$$\frac{dN}{dt}=-(C-B_1)N^3-B_0N^2\ , \tag{3}$$

where C is the unsaturated Auger recombination rate constant. Reasonable fits are obtained as $(C-B_1)$ is varied over the range $(1.5\text{–}3.0)\times10^{-29}$ cm^6/s and B_0 is correspondingly varied between $(0.3\text{–}1.0)\times10^{-10}$ cm^3/s. The best fit, shown by the solid line in Fig. 4, results from $C-B_1=2.0\times10^{-29}$ cm^6/s and $B_0=0.7\times10^{-10}$ cm^3/s. Using the relation $B_1/B_0=1.6\times10^{-19}$ cm^3 that has been measured for $\lambda_g=1.3$ μm In-Ga-As-P,[27] we obtain $C=3.1\pm1.0\times10^{-29}$ cm^6/s. This is in reasonable agreement with the range of values for the Auger coefficient reported in the literature.[4,5,24] The range of fit values of B_0 is comparable to literature values[5,24] at its high end. However, our data is not very sensitive to the value of B_0.

Recombination due to traps does not have to be invoked to explain the long-time decay. However, the data could also be fit with reasonable values of B and C and an additional term which has a decay rate of less than 4×10^7 s^{-1}, caused by recombination from traps. This is a reasonable upper bound, considering our films are uncapped, and so surface recombination is possible.

Another series of scans was taken again at delays of 200 ps to 3 ns for an initial density of 5×10^{20} cm^{-3} and a spot diameter of 5 μm. The carrier density at 200 ps is also roughly 5×10^{18} cm^{-3}, and the time evolution is the same as that observed with the lower initial carrier density. Qualitatively similar behavior for the long-time density decay was observed for the 0.6 μm thick film with $\lambda_g=1.3$ μm and the film with $\lambda_g=1.5$ μm.

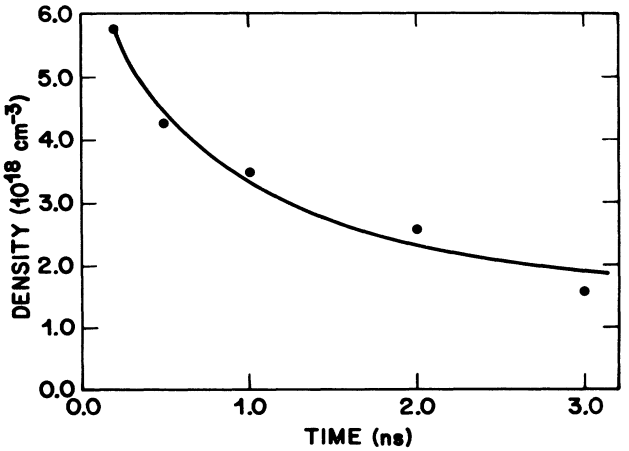

FIG. 4. Experimentally determined time evolution of the carrier density (points) for an initially photoexcited carrier density of 2.6×10^{19} cm^{-3} and an initial spot diameter of 26 μm. The solid line is the best fit to the data assuming Auger and radiative recombination, Eq. (3).

B. Band-gap renormalization

Next, consider a series of scans taken at a 200 ps delay with a 26 μm diameter excitation spot, with the initially excited carrier density varied from 2×10^{18} cm^{-3} to 2.6×10^{19} cm^{-3}. One result of this data is the variation of the band gap as a function of carrier density. The value of E_g that best fits each spectrum is shown in Fig. 5 as a function of fitted carrier density. The band gap decreases with increasing carrier density as predicted by the theory of band-gap renormalization.[7] The data is fit to the theoretical expression for $E_g(N)$ of the form:[28]

$$E_g(N)=E_g(0)-\gamma N^{1/3}\ . \tag{4}$$

Equation (4) considers the exchange interaction only, since the correlation energy is estimated to be more than 10 times smaller at these densities.[29] Furthermore, Eq. (4) is valid here since the thermal energy is small compared with the plasma energy. We obtain a value for γ of $(3.2\pm0.6)\times10^{-8}$ eV cm from the fit to the data in Fig. 5. Using the formalism described in Ref. 29 and appropriate parameters for In-Ga-As-P, we calculate a value for γ of 2.6×10^{-8} eV cm. To our knowledge, this quantity has not been previously measured in In-Ga-As-P. For GaAs γ has the measured value of 2.1×10^{-8} cm eV.[28] The good agreement between the data and the fit, as well as

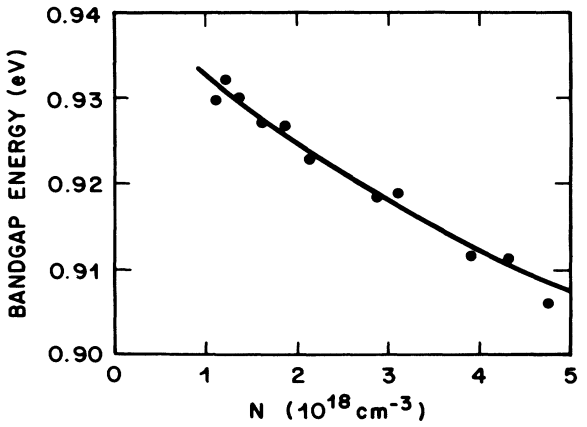

FIG. 5. Experimentally measured band-gap energy E_g as a function of carrier density N (solid circles). The solid line is a fit to the data using the theory of band-gap renormalization, Eq. (4).

the value for γ, support the hypothesis that the observed variation of band gap with carrier density is due to band-gap renormalization and is not an artifact of the line-shape fitting process.

C. Short-time decay (plasma expansion)

Our data show that even for initial carrier densities of up to 5×10^{20} cm^{-3} the carrier density at 200 ps is about 5×10^{18} cm^{-3}. During this initial period highly density-dependent decay mechanisms such as Auger recombination and plasma expansion should be dominant. (Pump-probe studies performed on thin In-Ga-As-P films with 0.5 ps resolution indicate that surface recombination is not an important decay mechanism during this initial period.[30]) To gain a qualitative understanding of the important decay mechanisms during this first 200 ps, consider the series of spectra shown in Fig. 2. Here, for a 5 μm photoexcited spot, the initial carrier density is varied from 5×10^{20} to 1.4×10^{20} cm^{-3} and spectra are taken at a delay of 200 ps. The spectra have roughly the same widths and shapes yielding carrier densities varying over a small range from 5.5×10^{18} to 4.7×10^{18} cm^{-3}. One might therefore expect roughly the same amount of luminescence intensity at 200 ps from these spectra. Their carrier distributions and densities are similar and the luminescence intensity depends on the instantaneous carrier distribution. (For these carrier densities the radiative recombination rate is beginning to saturate and the luminescence changes slightly less steeply than N^2.) However, the amount of luminescence changes by a factor of 3 although the carrier density changes only by a factor of 1.2. The initial carrier density, however, has changed by a factor of 3.5. The observed luminescence intensity at 200 ps depends on the *initial*, not the instantaneous, carrier density.

A mechanism for the density decay which provides a consistent explanation of the data is the expansion of the electron-hole plasma due to the highly density-dependent Fermi pressure.[8] Significant expansion occurs until a density is reached where the expansion rate becomes smaller than other decay mechanisms. Therefore, the larger the initially excited density, the larger the area of the plasma after 200 ps. For the present experiments, the expansion can be thought of as radial, since for thin films the density becomes uniform across the film in less than 0.5 ps.[30] The luminescence intensity is thus proportional to the excited area (assuming for simplicity a uniform carrier density over the area of the plasma). Therefore, for a given instantaneous carrier density, the instantaneous luminescence should increase with increasing initial carrier density if significant plasma expansion has occurred. This occurs because, although carrier density decreases because of expansion, the carriers are not lost and hence are able to contribute to the luminescence. By 200 ps after excitation, the carrier density is low enough that the dominant loss mechanisms should be Auger and bimolecular radiative recombination. This is supported by the time-delay data of Fig. 4. Hence the dominance of plasma expansion as the density decay mechanism lasts less than 200 ps.

More quantitative evidence of plasma expansion lies in examination of L_0 as a function of initially photoexcited density. Assuming a uniformly excited region, L_0 is independent of photon energy and carrier density and will be proportional to the area of the region. A plot of L_0 versus initial carrier density N_0 is shown in Fig. 6(a) (circles), for the data from the 5 μm initial spot diameter (Fig. 2). That L_0 increases with initial density means that the spot size at a delay of 200 ps also increases with initial density. Therefore, this data tends to indicate that expansion of the photoexcited electron-hole plasma occurred and that the higher the initial density the larger the expansion. This is consistent with an expansion of the plasma driven by the Fermi pressure. In Fig. 6(b) we plot L_0 versus N_0 for a series of spectra with a 26 μm diameter spot size and a delay of 200 ps. Again, L_0 increases with N_0, indicating that plasma expansion has occurred even under these less dense initial conditions. In Fig. 6(c), L_0 versus delay is plotted for the series of spectra shown in Fig. 1 taken with an initial spot size of 26 μm and an initial density of 2.6×10^{19} cm^{-3}. That L_0 remains constant with time delay indicates that there is no plasma expansion after the first 200 ps. Additional data from time-resolved transmission and reflection experiments[30] with 0.5 ps resolution suggest that plasma expansion may occur within 20 ps after the excitation.

Another possible explanation for the anomalously large change in luminescence intensity corresponding to a small change in the spectral width consists of postulating a very low Γ-L valley splitting,[4] $E_{\Gamma L}$ of ≈0.14 eV instead of the estimated splitting of 0.55 eV. Under these conditions, carrier densities of $\approx5\times10^{18}$ cm^{-3} would begin to fill the L valleys. Since there are four equivalent valleys with large masses ($0.328m_0$) and since the heavy-hole mass is also large, the spectral width would not be a sensitive measure of carrier density in this region. Although electrons in the L valley do not contribute to luminescence the holes can still contribute. Therefore, the amount of luminescence will still increase with increasing initial car-

rier density. The spectral shapes can be fit under these assumptions. However, to explain the observed large luminescence intensity change requires not only a very low value of $E_{\Gamma L}$ but also much larger values of the L-valley masses than estimated.[17] These values seem physically unreasonable and, therefore, we reject this hypothesis as an explanation of our data.

In order to investigate the plasma expansion hypothesis we made a measurement of the size of the luminescing spot at 200 ps delay. Luminescence from the sample was collected with a 20× microscope objective and collimated.

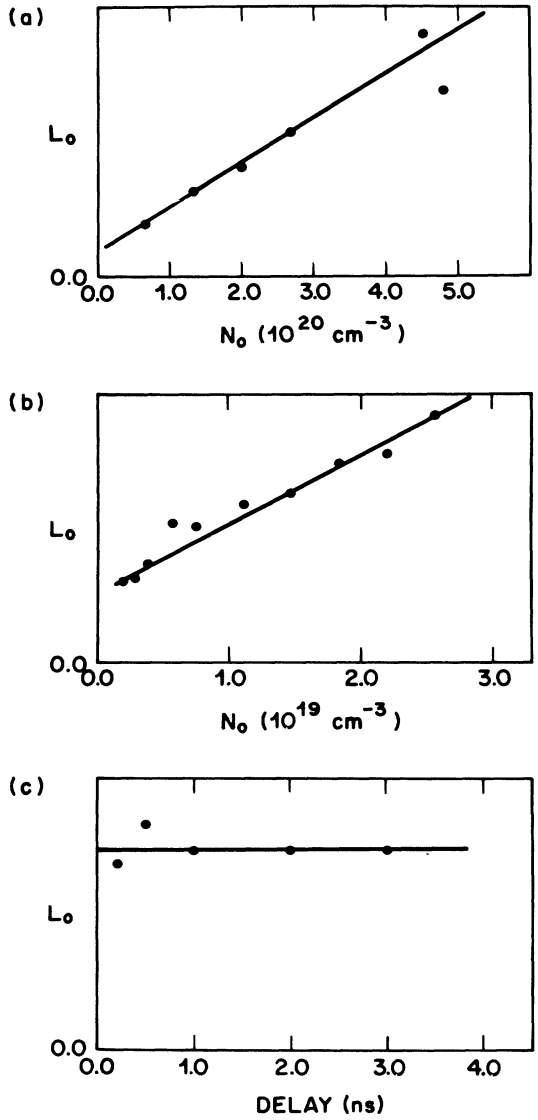

FIG. 6. Experimentally determined L_0 as a function of initially photoexcited density N_0 (solid circles) for an initial spot diameter of 5 μm (a) and 26 μm (b). Experimentally determined L_0 as a function of delay for an initial density of 2.6×10^{19} cm^{-3} and 26 μm spot diameter (c). The solid lines serve as a guide to the eye.

After removing any residual laser light with a filter, the collimated beam was refocused with another 20× objective to form a 1:1 image. The size of this imaged spot is determined by measuring the amount of light transmitted through various calibrated pinholes. (A Gaussian beam was assumed for results reported here. However, the data was interpreted for several different assumed beam shapes and the same general trends were observed.) By using the sampling oscilloscope in boxcar averaging mode, as described earlier, the spot size is measured at a 200 ps delay from photoexcitation. For this measurement the excitation spot size was 5 μm. A series of spot-size measurements at different values of N_0 for comparison with the L_0 versus N_0 data of Fig. 6(a) were made. This data is presented in Fig. 7 (crosses) along with the data of Fig. 6(a) (circles). Since L_0 is merely a relative measure of area, a comparison of the slopes of the two sets of data is relevant. The L_0 versus N_0 data has been normalized to match the area data at high values of N_0. The horizontal dash-dotted line at the bottom of the graph (area 0.2×10^{-6} cm^2) indicates the area of the initially excited spot. The area measurements therefore do show that significant expansion has occured. A factor of 25 increase in area has occured for $N_0=5\times10^{20}$ cm^{-3}, indicating that the density has decreased to $\approx2\times10^{19}$ cm^{-3} at a delay at 200 ps due to plamsa expansion alone. The measured value of the density at 200 ps is $\approx5\times10^{18}$ cm^{-3}. Therefore, a significant amount of the density decay is probably due to plasma expansion. There is an $\sim35\%$ difference between the measured change of area with N_0 and that indicated by the L_0 versus N_0 measurements. This could be due to the fact that the density is not uniform over the spot as assumed in the interpretation of the L_0 measure-

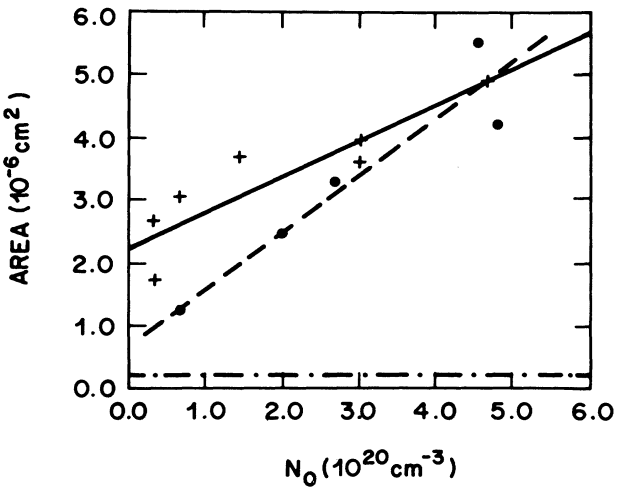

FIG. 7. Measurement of luminescing spot area. The crosses are measurements of the luminescing spot area 200 ps after excitation as a function of initial carrier density. The solid circles are area measurements obtained from L_0 vs N_0 measurements [Fig. 6(a)]. The solid circles have been normalized to match the crosses at high values of N_0. The horizontal dash-dotted line shows the area of the initially excited spot.

ments. It could also indicate that the high point in the L_0 data (at $N_0=4.5\times10^{20}$ cm^{-3}) is "bad," as the agreement between the two sets of data would be better without that data point.

To prevent plasma expansion from occurring, we tried to confine the photoexcited carriers in small pieces of In-Ga-As-P films with transverse dimensions comparable to the focal spot size (<10 μm). Unfortunately, the cleaved faces on the edges of these films provided enough feedback that these photoexcited films lased in the transverse direction. The luminescence spectra obtained at the minimum delay of 200 ps showed the ~100 meV spectral width seen from the larger area films with an additional strong peak due to scattered light at the lasing frequency. In this case, a decay of the carrier density has occured in a time much less than 200 ps because of stimulated emission.

D. Rate equation analysis

Auger recombination has been observed to be the major cause of carrier decay in other studies of dense electron-hole plasmas in In-Ga-As-P (Refs. 2, 4, 5, 24, and 31) or In-Ga-As (Refs. 24, 25, and 32). In all these experiments, excitation was at a wavelength of 1.06 μm or longer, so that carrier densities as high as 1×10^{20} cm^{-3} could not be attained. Also, focal spot sizes as small as 5-μm diameter were not used in any of those studies. The conditions of high initial carrier density and small spot size both tend to emphasize plasma expansion. In the section that follows, the relative significance of Auger recombination versus plasma expansion will be evaluated using a very simple rate-equation analysis.

Plasma expansion is driven by a spatial gradient in the chemical potential of the electron-hole plasma, due to a spatial gradient of carrier density. Even in one dimension, the mathematics is extremely complex.[8] In Combescot's hydrodynamic model for plasma expansion, a single, initial sharp discontinuity in plasma density evolves into a nonuniform distribution of density. For simplicity, in our model we will assume that the plasma density is constant within its boundary, but its boundary increases with time. Our model violates the principles of hydrodynamics, but it leads to tractable expressions.

Combescot's model, which relies on a highly density-dependent Fermi pressure assumes that $T=0$. A simple calculation of the Fermi pressure at $T=300$ K was made for the present system following Ref. 29. We find that the Fermi pressure at a density of 10^{20} cm^{-3} is ≈2000 times larger than at 10^{18} cm^{-3}, leading us to believe that for the high densities here a finite temperature does not change the qualitative features of the calculation.

First, consider plasma expansion with no additional decay mechanisms. The plasma has filled the thickness of the film in less than 0.5 ps,[30] so the expansion is two-dimensional. The density of the plasma $N(t)$ at time t is

$$N(t)=\frac{N_T}{\pi dr^2}\ , \tag{5}$$

where N_T is the total *number* of carriers in the plasma, d is the thickness of the film, and r is the time-dependent radius of the plasma (r_0 at $t=0$). For mathematical convenience, we assume that the radius of the plasma expands at a rate given by Eq. (6):

$$\frac{dr}{dt}=a(N-N^*)^{1/2}\ , \tag{6}$$

where N^* is the equilibrium density of the plasma[8] and a is a constant to be defined. We will take $N^*=5\times10^{18}$ cm^{-3} for In-Ga-As-P, because this density is observed at 200 ps delay regardless of initial excitation density (Fig. 2). Combescot derives, for the case where $N>N^*$, an expansion velocity for the boundary of the plasma that is proportional to $\ln(N/N^*)$. The logarithmic function and the square root used in Eq. (6) are similar curves. The decay of carrier density due to plasma expansion can be obtained by differentiating Eq. (5) and using Eq. (6):

$$\frac{dN}{dt}=-DN^2\left[1-\frac{N^*}{N}\right]^{1/2}\ , \tag{7}$$

where $D=2a\sqrt{\pi d/N_0}$. It is assumed for the present that no carriers are lost because of plasma expansion ($dN_T/dt=0$). Equation (7) can be integrated and solved to find the time, τ_E, at which, due to plasma expansion, $N=N^*$. The result is

$$\tau_E=\frac{1}{DN^*}\left[1-\frac{N^*}{N_0}\right]^{1/2}\ . \tag{8}$$

In what follows, the data for the tight focus will be considered. For this data $N^*/N_0\ll1$, and $\tau_E=1/DN^*$.

For high-carrier densities in In-Ga-As-P, the band-to-band radiative recombination rate saturates. As an approximation to the detailed calculations of Sermage and co-workers,[5] valid in the intermediate- and high-density regimes under consideration here, the following form is used for the radiative recombination rate

$$\left[\frac{dN}{dt}\right]_{\rm rad}=\frac{B_0}{\delta}(1-e^{-\delta N})N\ . \tag{9}$$

The detailed calculations[5] are fit by the values $B_0=1.4\times10^{-10}$ cm^3/s and $\delta=1.8\times10^{-19}$ cm^3 for a temperature of 300 K.

Now consider the combined effects of plasma expansion and decay due to Auger and radiative recombination. For the decay of density due to plasma expansion, Eqs. (7) and (8) are used and the terms containing N^*/N are neglected. The result is

$$\frac{dN}{dt}=-CN^3-DN^2-\frac{B_0}{\delta}(1-e^{-\delta N})N\ . \tag{10}$$

The first term on the right-hand side is due to unsaturated Auger recombination. At the high densities, the radiative recombination term is insignificant compared to the other two terms, and is neglected. Equation (10) is solved implicitly for $N(t)$ by

$$\frac{1}{N}-\frac{1}{N_0}+\frac{C}{D}\ln\left[\frac{C+D/N_0}{C+D/N}\right]=Dt\ . \tag{11}$$

The plasma expands according to Eq. (6), where the value of N is obtained from Eq. (11). Thus, the area $A(t)$ is given by

$$A(t)=\pi r(t)^2 , \tag{12}$$

where

$$r(t)=r_0+\frac{D}{2}\left[\frac{N_0}{\pi d}\right]^{1/2}\int_0^t (N-N^*)^{1/2}dt .$$

The expansion stops when $N=N^*$.

The total luminescence intensity at time t is obtained, using Eq. (9):

$$L(t)=\beta\frac{B_0}{\delta}(1-e^{-\delta N})NA(t)d , \tag{13}$$

where β is a constant describing collection efficiency, etc. Comparing Eqs. (13) and (2), L_0 is seen to be proportional to $A(t)$. In using Eq. (13), N and A are calculated from Eqs. (11) and (12).

The case of carrier decay by Auger and radiative recombination with no plasma expansion can also be examined. The rate equation for high density, where the radiative recombination rate is saturated, is

$$\frac{dN}{dt}=-CN^s-\frac{B_0}{\delta}N . \tag{14}$$

Saturation of the Auger recombination rate[25] is accounted for by the value of the exponent s ($3\geq s\geq 2$, and $s=3$ corresponds to unsaturated Auger recombination). Equation (14) is solved by

$$N=\epsilon^{s-1}\left[\left[1+\frac{\epsilon}{N_0^{s-1}}\right]\exp\left[\frac{(s-1)B_0t}{\delta}\right]-1\right] , \tag{15}$$

where $\epsilon=B_0/C\delta$. The luminescence intensity at time t is given again by Eq. (13), using Eq. (15) and a constant value for A.

The luminescence intensity 200 ps after excitation was calculated for three cases: (1) unsaturated Auger decay and plasma expansion, Eqs. (11)–(13), (2) unsaturated Auger recombination without plasma expansion, Eqs. (13) and (15) with $s=3$, and (3) saturated Auger recombination without plasma expansion, Eqs. (13) and (15) with $s=2.16$.[25] For cases (1) and (2), the value[5] $C=2.6\times10^{-29}$ cm^6/s was used. For case (1), the expansion time τ_E was taken to be either 10 or 100 ps, so $D=2.0\times10^{-8}$ cm^3/s or 2.0×10^{-9} cm^3/s. For case (3), we take $s=2.16$ and $C=8\times10^{-14}$ cm$^{3.48}$/s. The exponent is the same as that found by Sermage *et al.*[25] for the saturated Auger process in In-Ga-As (for $N>2.5\times10^{18}$ cm^{-3}). We use a value of C that is 2.5 times smaller than that found for In-Ga-As, since the unsaturated Auger coefficient for 1.3 μm In-Ga-As-P is 2.5 times smaller than that for In-Ga-As.[5,25]

The results of the calculations are compared to experiment in Fig. 8. The data points are for luminescence intensity at 200 ps versus initial excitation density for the 5 μm diameter spot, as in Figs. 6(a) and 7. The model that includes plasma expansion, case (1), shows an approximately linear increase in luminescence at 200 ps as a function of initial excitation density. Neither model which includes Auger recombination but not plasma expansion, cases (2) and (3), can adequately explain the data. The curves for case (1) obtained with $D=2\times10^{-8}$ cm^3/s and $D=2\times10^{-9}$ cm^3/s are almost indistinguishable. For either value of D, the major cause of carrier density decay during the first 200 ps after photoexcitation is plasma expansion. Auger recombination causes only $\approx$20–30% of the carrier density decrease. The relative insignificance of Auger recombination occurs because the plasma expands rapidly, causing the density to decrease rapidly. Once the expansion slows down, the density is already below $\approx10^{19}$ cm^{-3}, and the Auger rate is much slower than it would be at the much higher initial densities.

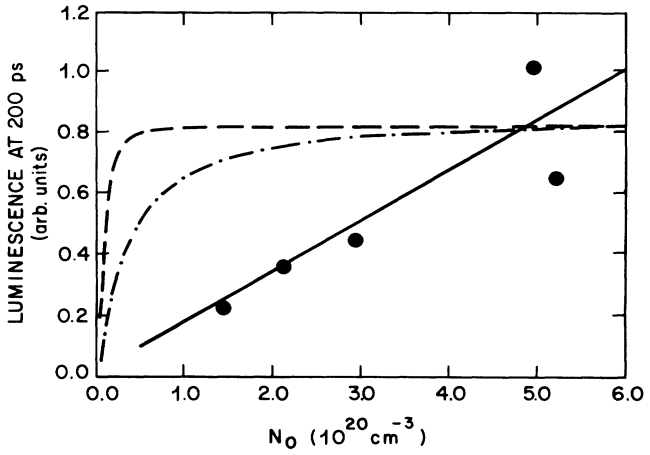

FIG. 8. Calculated luminescence intensity 200 ps after excitation as a function of initial carrier density, assuming: (1) plasma expansion with unsaturated Auger recombination (solid line), (2) unsaturated Auger recombination without plasma expansion (dashed line), or (3) saturated Auger recombination without plasma expansion (dash-dotted line). The solid circles are measured data points for the luminescence intensity at 200 ps for an initial 5 μm diameter spot, as in Fig. 6(a).

Case (2), the model for unsaturated Auger recombination, predicts that the carrier density 200 ps after photoexcitation will be 8×10^{18} cm^{-3} regardless of initial excitation density, for initial densities greater than 3×10^{19} cm^{-3}. For this reason, the luminescence intensity at 200 ps is also independent of N_0 above 3×10^{19} cm^{-3}. Case (3) shows some variation in carrier density at 200 ps with initial excitation density. However, for case (3) also, the luminescence intensity at 200 ps is not very dependent on initial excitation density for N_0 above 1×10^{20} cm^{-3}.

Although the rate equation model for plasma expansion is not rigorous, it does suggest that plasma expansion can explain both the increase in luminescence intensity with increasing N_0 and the constant value of N at 200 ps delay. It also suggests that Auger recombination which

occurs simultaneously with plasma expansion need not be a major source of carrier density decay. The results shown in Fig. 8 indicate that Auger recombination alone cannot be reconciled with the increase in luminescence at 200 ps as the initial carrier density is increased.

If, as suggested by the data and rate-equation analysis, the dominant density decay mechanism during the first 200 ps is plasma expansion, then, for the highest initial density of 5×10^{20} cm^{-3}, the plasma expands with an average radial velocity of $>10^7$ cm/s. If this plasma expansion occurs in the first 20 ps after excitation, as suggested by the pump-probe experiments of Ref. 30, then an expansion velocity of $\sim10^8$ cm/s is implied. This speed is comparable to the Fermi velocity. Other works have indicated that plasma expansion in GaAs can also occur at speeds of 10^7 cm/s.[13,14] In contrast, plasma expansion in the II-VI compounds CdS and CdSe appears to occur with a slower velocity of 10^6 cm/s.[11,12] For GaAs and In-Ga-As-P, the rapid plasma expansion occurs in competition with Auger recombination. However, the Auger recombination coefficient for GaAs (Ref. 33) is 1 to 2 orders of magnitude smaller than that of In-Ga-As-P. It is therefore interesting that in spite of the larger Auger coefficient for 1.3 μm In-Ga-As-P, plasma expansion can be the dominant mechanism for carrier density decay. For the material $GaAs_{0.62}P_{0.38}$, plasma expansion after excitation in a small spot can also occur,[9] in spite of a large Auger coefficient measured to be 3×10^{-29} cm^6/s,[26] (a value close to that of $In_{0.70}Ga_{0.30}As_{0.66}P_{0.34}$).

V. CONCLUSIONS AND SUMMARY

Regardless of the initial excitation density, up to 5×10^{20} cm^{-3}, a decrease in carrier density to $<6\times10^{18}$ cm^{-3} occurs in In-Ga-As-P films within 200 ps after excitation by 0.5 ps, 2.0 eV pulses. A rate-equation model indicates that Auger and bimolecular radiative recombination are not the dominant mechanisms for this initial decay of plasma density. Expansion of the electron-hole plasma at a speed $>10^7$ cm/s provides a possible explanation for the observed data. The observed decay of density after 200 ps is dominated by Auger and bimolecular radiative recombination. Values derived for the rate constants for these processes are comparable to those measured by other groups.[4,5,24] The carriers are found to equilibrate to a temperature near the lattice temperature within 200 ps after excitation. Band-gap renormalization due to the dense electron-hole plasma has been measured.

ACKNOWLEDGMENTS

We thank J. Stone, A. G. Dentai, and J. F. Ferguson for supplying the samples used in this work. We are grateful to J. Stone, N. K. Dutta, and T. P. Pearsall for helpful discussions.

*Present address: Los Alamos National Laboratory, Los Alamos, NM 87545.

[1]K. Kash and J. Shah, Appl. Phys. Lett. **45**, 401 (1985).
[2]J. C. V. Mattos, E. O. Gobel, and A. Mozer, Solid State Commun. **55**, 811 (1985).
[3]K. Kash, D. Block, and J. Shah, Phys. Rev. B **33**, 8762 (1986).
[4]B. Sermage, H. J. Eichler, J. P. Heritage, R. J. Nelson, and N. K. Dutta, Appl. Phys. Lett. **42**, 259 (1983).
[5]B. Sermage, J. P. Heritage, and N. K. Dutta, J. Appl. Phys. **57**, 5443 (1985).
[6]J. M. Wiesenfeld and J. Stone, IEEE J. Quantum Electron. **QE-22**, 119 (1986).
[7]W. F. Brinkman and T. M. Rice, Phys. Rev. B **7**, 1508 (1973).
[8]M. Combescot, Solid State Commun. **30**, 81 (1979).
[9]J. Modest, A. Frava, J. L. Staehli, M. Guzzi, and M. Capizzi, Phys. Status Solidi B **108**, 281 (1981).
[10]A. Cornet, T. Amand, M. Pugnet, and M. Brousseau, Solid State Commun. **43**, 147 (1982).
[11]F. A. Majumder, H. E. Swoboda, K. Kempf, and C. Klingshern, Phys. Rev. B **32**, 2407 (1985).
[12]H. Saito and E. Gobel, Phys. Rev. B **31**, 2360 (1985).
[13]K. M. Romanek, H. Nather, J. Fischer, and E. O. Gobel, J. Lumin. **24-25**, 585 (1981).
[14]A. Forchel, H. Schweizer, and G. Mahler, Phys. Rev. Lett. **51**, 501 (1983).
[15]H. Burkhard, H. W. Dinges, and E. Kuphal, J. Appl. Phys. **53**, 655 (1982).
[16]E. O. Kane, J. Phys. Chem. Solids **1**, 269 (1957).
[17]M. A. Littlejohn, T. H. Glisson, and J. R. Hauser, in *Ga-In-As-P Alloy Semiconductors,* edited by T. P. Pearsall (Wiley, New York, 1982), p. 257.
[18]K. Alavi, R. L. Aggarwal, and S. H. Groves, Phys. Rev. B **21**, 1311 (1980).
[19]C. Hermann and T. P. Pearsall, Appl. Phys. Lett. **38**, 450 (1981).
[20]P. M. Laufer, F. H. Pollak, R. E. Nahory, and M. A. Pollack, Solid State Commun. **36**, 978 (1980).
[21]K. Y. Cheng, A. Y. Cho, S. B. Christman, T. P. Pearsall, and J. E. Rowe, Appl. Phys. Lett. **40**, 423 (1982).
[22]R. J. Nicholas, J. C. Portal, C. Houlbert, P. Perrier, and T. P. Pearsall, Appl. Phys. Lett. **34**, 492 (1979).
[23]T. Amand and J. Collet, J. Phys. Chem. Solids **46**, 1053 (1985).
[24]E. Wintner and E. P. Ippen, Appl. Phys. Lett. **44**, 999 (1984).
[25]B. Sermage, D. S. Chemla, D. Sivco, and A. Cho, IEEE J. Quant. Electron. **QE-22**, 774 (1986).
[26]H. J. Zarrabi, W. B. Wang, and R. R. Alfano, Appl. Phys. Lett. **46**, 513 (1985).
[27]C. B. Su, R. Olshansky, J. Manning, and W. Powazinik, Appl. Phys. Lett. **44**, 732 (1984).
[28]J. Shah, R. F. Leheny, and C. Lin, Solid State Commun. **18**, 1035 (1976).
[29]S. Tanaka, H. Yoshida, H. Saito, and S. Shionoya, in *Semiconductors Probed by Ultrafast Laser Spectroscopy,* edited by R. R. Alfano (Academic, Orlando, 1984), Vol. 1, p. 172.
[30]J. M. Wiesenfeld and A. J. Taylor, Phys. Rev. B **34**, 8740 (1986).
[31]A. Miller, R. J. Manning, A. M. Fox, and J. H. Marsh, Electron. Lett. **20**, 601 (1984).
[32]M. E. Prise, M. R. Taghizadeh, S. D. Smith, and B. S. Wherrett, Appl. Phys. Lett. **45**, 652 (1984).
[33]G. Benz and R. Conradt, Phys. Rev. B **16**, 843 (1977).